INF.2

Economic and Social Council

Inland Transport Committee

7 November 2023

Original: English

Working Party on the Transport of Dangerous Goods

Joint Meeting of Experts on the Regulations annexed to the European Agreement concerning the International Carriage of Dangerous Goods by Inland Waterways (ADN) (ADN Safety Committee)

Forty-third session
Geneva, 22-26 January 2024
Item 5(b) of the provisional agenda
Proposals for amendments to the Regulations annexed to ADN: other proposals

Proposed changes to 9.3.4 of ADN

Transmitted by the Recommended ADN Classification Societies

Annexes to document ECE/TRANS/WP.15/AC.2/2024/11

Annex I

Revision ADN 9.3.4. Summary and Recommendations

TNO Public ⟩ TNO 2023 R10366
18 May 2023

Mobility & Built Environment
www.tno.nl

TNO 2023 R10366 – 18 May 2023

Revision ADN 9.3.4. Summary and Recommendations

Author(s)	M.G. Hoogeland M.L. Deul N.P.M. Werter O.J. Coppejans R.P. Sterkenburg A.W. Vredeveldt

Classification report	TNO Public
Title	TNO Public
Report text	TNO Public
Appendices	TNO Public
Number of pages	26 (excl. front and back cover)
Number of appendices	2
Sponsor	Revision ADN 9.3.4. consortium
Project name	Revision ADN 9.3.4.
Project number	060.43088

Contents

1 Introduction

Design and operation of inland waterway ships carrying dangerous goods are with regard to safety regulated in the European Agreement concerning the International Carriage of Dangerous Goods by Inland Waterways (ADN). ADN features a section 9.3.4 called Alternative Constructions. This section describes how cargo tanks exceeding the default ADN maximum size of 380 m^3 can still be permitted through providing for additional protection against collisions.

Section 9.3.4 was written in 2005 and based on knowledge and know-how available at that time. At some points this knowledge and know-how have become outdated. Therefore an investigation was carried out by TNO together with industrial parties aimed at revising and updating the text of section 9.3.4 in accordance with the current state of the art.

Section 9.3.4 also states a maximum allowable tank size of 1000 m^3. At the initiation of the revision/update the question was raised whether this value could be increased. The main reason for this is the introduction of alternative fuels in inland waterway shipping, e.g. LNG and hydrogen, requiring dedicated tankers for transporting these fuels which would benefit from tanks exceeding the 1000 m^3 limit. Therefore the investigation also included work on the associated risk implications of exceeding this 1000 m^3 limit.

1.1 Issues addressed

There are three categories of issues which have been addressed in this investigation:

1. Collision energy currently available on the river to inflict damage to other ships.
2. Guidelines on how to conduct collision crash calculations.
3. The upper limit of tank size at 1000 m^3.

The shipping statistics used for the collision energy cumulative probability density functions used in the current text of section 9.3.4 are from 1999. The functions are now updated based on 2018 shipping statistics.

Over the past two decades much experience has been gained in conducting crash calculations on ship structures. This includes experience with two different explicit finite element packages, which are used for such calculations. This experience is used to formulate an update of the guidelines for crash calculations.

The feasibility of increasing the maximum tank size beyond the current 1000 m^3 limit has been investigated through loss of containment effect analyses for tank sizes up to 5000 m^3.

These three issues are reported in separate background documents. The summary is provided in this report per issue. The recommendations resulting from the investigations are given Chapter 5.

1.2 References

This work refers to five external documents, while the results are reported in three TNO documents.

1.2.1 External documents

[1] ADN, European Agreement concerning the International Carriage of Dangerous Goods by Inland Waterways as from 1 January 2021, ECE/TRANS/301 (Vol. I & II), https://unece.org/adn-2019-files
[2] Driving Dynamics of Inland Vessels, 2016 Bundesanstalt für Wasserbau (BAW), Karlsruhe, Germany
[3] EFFECTS version 11.5.1.21121, A computer program to calculate the physical effects and consequences of the escape of hazardous chemicals, Gexcon, 2021
[4] https://www.scenarioboekev.nl/ (accessed 2021)
[5] https://www.infomil.nl/onderwerpen/veiligheid/basisnet/ (accessed 2021)

1.2.2 TNO reports

[6] TNO 2022 R12238, Background document: Updated ADN 9.3.4 collision energy statistics
[7] TNO 2022 R11532, ADN 9.3.4 FE Sensitivity Analysis
[8] TNO 2022 R10765, Revision ADN 9.3.4 - WP Consequence Analysis

1.2.3 Acknowledgements

The work performed has been done with the sponsoring and in kind contributions of the following partners:

Annmar Engineering
Bureau Veritas
Damen Naval Shipyards
Femto Engineering
GTT
Lloyds Register of Shipping
Mercurius
Oudcomb
Rensen Driessen
Somtrans
TNO
Victrol

2 Issue 1: Collision energy

In the current ADN section 9.3.4 (ref [1]), the probabilities of a collision exceeding a chosen collision energy level are based on 1999 shipping statistics. Since then the population of ships has increased significantly. Moreover there has been a shift towards ships with larger displacements, due to the introduction of 100 m and 135 m ships. As a consequence, energy available on the river to inflict collision damage has increased. Therefore the cumulative probability density functions for collision energies have to be updated. A full report can be found in [6].

2.1 Approach

The collision energy that a struck ship will absorb in a collision depends on the mass and velocity of the striking ship, its own mass and the collision velocity. It is reasonable to assume a fully inelastic collision and for the struck ship an initially zero lateral velocity. Under these assumptions the absorbed energy equals:

$$E_{diss} = \frac{1}{2} m_a v_a^2 \left(\frac{m_b}{m_a + m_b}\right) \qquad (1)$$

With : E_{diss} collision energy absorbed by the structure [kJ]
m_a effective mass of striking ship [tonnes]
m_b effective mass of struck ship [tonnes]
v_a velocity of striking ship [m/s]

The displacement of the striking ship is multiplied by 1.1 to obtain the effective mass, i.e. including added mass longitudinal direction. The displacement of the struck ship is multiplied by 1.4 in order to include added mass in lateral direction. In order to determine a probability distribution of collision energies both ship masses and collision velocity must be known.

2.2 Main findings collision energy statistics

2.2.1 Ship masses

Figure 2.1 shows the number of ship passages per effective mass class observed in 2017. The largest effective mass of a single unit observed is 15,500 tonnes (including added mass). Effective mass ranges were chosen in bins of 500 tonnes for a finer distribution of ship masses. The range is extended to the largest registered mass on the river.

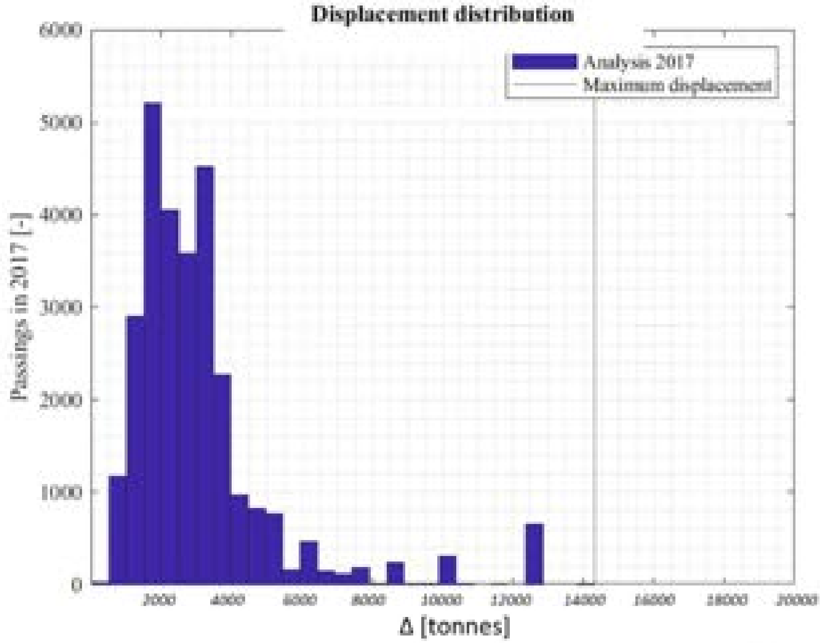

Figure 2.1 Ship passages per effective mass classes, 2017

Most passages are in the effective mass range between 1000 and 5000 tonnes. Additionally, there were slightly under 700 passages in the 12,000 – 14,000 tonnes effective mass range, to be attributed to push barge convoys carrying iron ore and coal.

2.2.2 Collision velocities

Collision velocities in regulation 9.3.4. are based on maximum sailing velocities. For each ship type these are taken from data published by Bundesanstalt für Wasserbau (BAW, ref [2]). It is noted that the ships sailing independently can sail at speeds as high as 18 km/hr. Push convoys tend to sail at 14 km/hr.

2.2.3 Energy distribution

The collision energies for given ship masses and ship velocities can be determined by eq. (1). Figure 2.2 and Figure 2.3 show the results. In this case, an infinite effective mass of the struck ship was assumed (viz. moored alongside a quay). This implies all energy would need to be absorbed by the struck ship in case of a collision. There is no energy in the sway motion of the struck ship. The figures are intended to show the difference between 1999 and 2017. Two histograms are shown. Figure 2.2 depicts the probability density function of kinetic energies available on the river in terms of single ships. Figure 2.3 shows the associated cumulative probability density functions (CPDF) derived for 1999 and 2017 data. Data is shown for both the 1999 situation (red) and the 2017 situation (blue). As can be seen, higher collision energies are available in the 2017 case. Figure 2.2 and Figure 2.3 show that there is a clear need to update ADN regarding collision energy statistics.

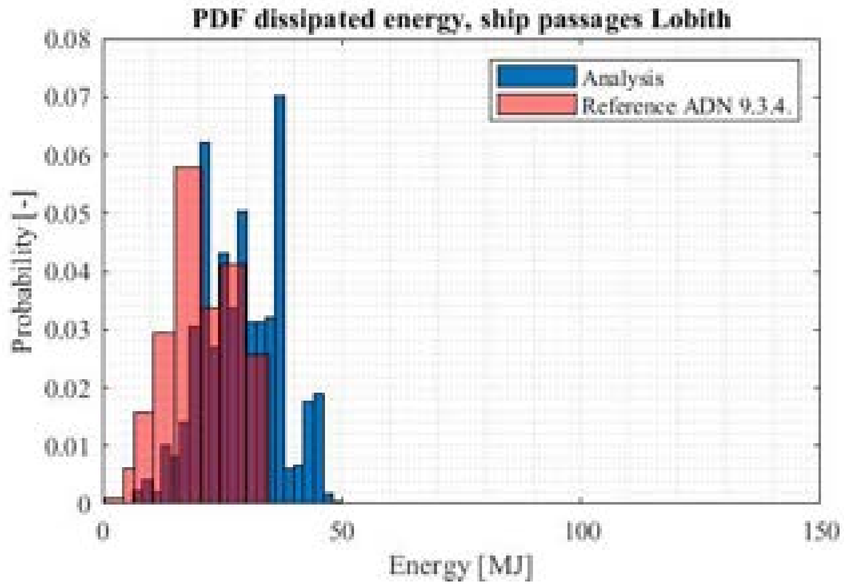

Figure 2.2 Probability density of collision energy river Rhine (1999 and 2017)

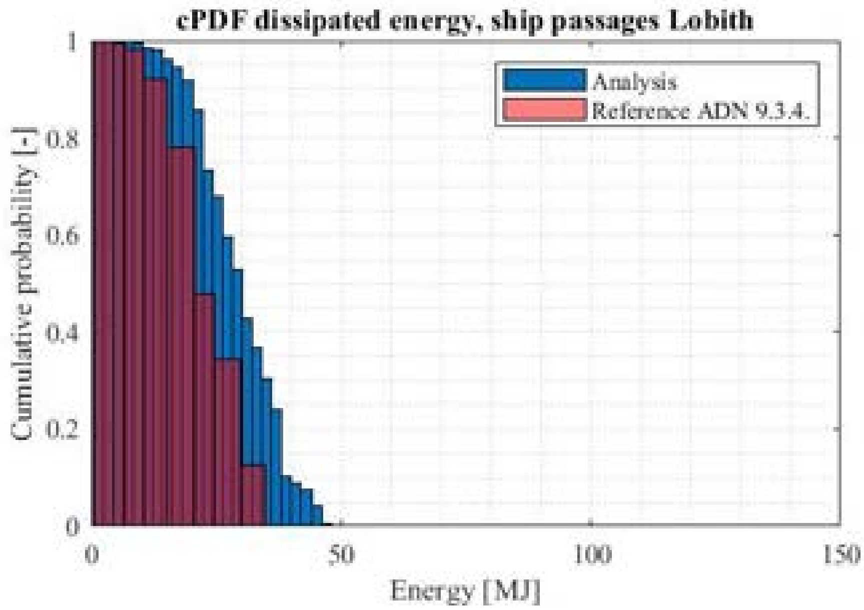

Figure 2.3 Cumulative probability density of collision energy river Rhine (1999 and 2017)

According to equation (1), the collision energy available to cause damage to a struck ship also depends on the mass of the struck ship. Hence the CPDF for collision energy depends on the mass of the struck ship as well. Therefore, in order to illustrate the consequences for an actual collision case where the struck ship is allowed to sway, a mass has to be assumed for the struck ship.

Figure 2.4 shows an example of such a curve (including tabulated figures) for a struck ship with an effective mass of 8000 tonnes. For comparison purposes the curve used in de current ADN 9.3.4 regulation is shown as well.

As expected the available collision energy to inflict damage has increased significantly since 1999.

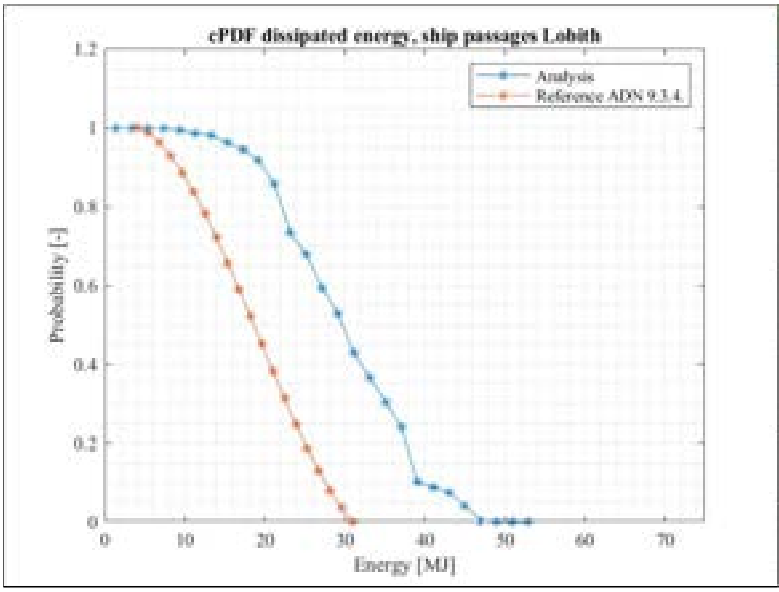

8000 tonnes	
E coll [MJ]	CPDF [-]
3.39	1.000
5.37	0.999
7.35	0.999
9.34	0.995
11.32	0.986
13.30	0.982
15.28	0.962
17.26	0.946
19.25	0.918
21.23	0.858
23.21	0.734
25.19	0.680
27.17	0.595
29.16	0.529
31.14	0.429
33.12	0.367
35.10	0.305
37.09	0.241
39.07	0.102
41.05	0.089
43.03	0.076
45.01	0.041
47.00	0.004
48.98	0.001
50.96	0.000
52.94	0.000

Figure 2.4 CPDF collision energy, struck vessel 8000 Tonne, 2018 statistics vs 1999 statistics

2.3 Discussion collision energies

The consequence of the updated collision energy CPDF is shown in Figure 2.5. As a typical example, the consequence of a ship with 760 m^3 tanks is taken. In this case the tank size is double the allowable maximum volume stipulated in ADN. According to ADN 9.3.4., doubling the tank size requires a ship with a crashworthiness which will reduce the probability tank rupture by half compared to a ship designed in compliance with the prescriptive regulations for scantlings according ADN (the minimum scantlings design or reference design).

Suppose the reference design is able to absorb 20 MJ prior to tank rupture. Based on the 1999 data the probability of tank rupture, given a collision, is approx. 0.43. The new design would therefore require a probability reduction down to 0.43/2 = 0.215. Based on the 1999 curve an energy absorbing capacity of 24.5 MJ would be required to attain this probability reduction.

The same exercise based on the 2017 curve yields a rupture probability for the reference design of 0.88. So now the probability must be reduced to 0.88/2 = 0.44 for the new design. The CPDF curve shows that this requires an energy absorbing capacity of at least 31 MJ.

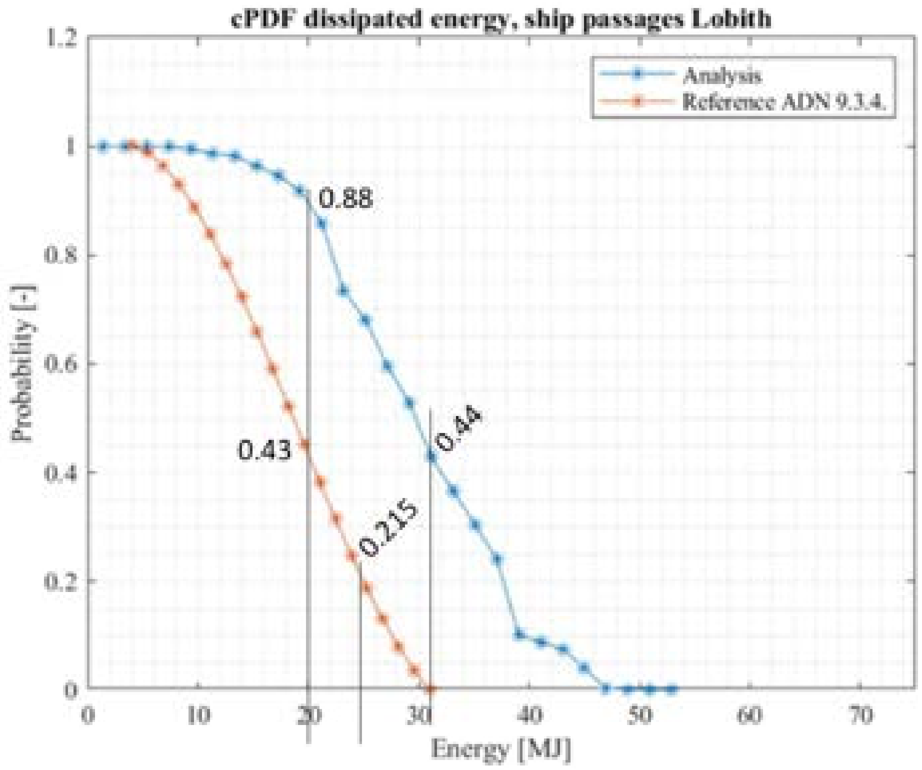

Figure 2.5 Consequence of updated energy statistics

2.4 Recommendations

From the updated energy statistics, the following recommendations arise:

- Update the cumulative probability density curves as indicated in this section.
- List the values of the cumulative probability density curves in tables instead of formulas.
- Give tabled values for effective ship mass classes from 1500 to 14,000 tonnes, with 500 tonnes steps up to 4000 tonnes, larger steps between 5000 and 14,000 tonnes.

3 Issue 2: Guidance on crash calculations

Section 9.3.4 from the ADN prescribes how the crash calculations to obtain the energy absorbing capacity of the ship structure need to be carried out. Calculations must be done by explicit finite element methods such as Abaqus and LS-Dyna. For running these analyses many assumptions and choices have to be made for which recommendations are given. The validity of these recommendations has been investigated further in this project.

Experience with crash calculations in the past shows that sometimes structural material trapped between the striking bow and tank causes unconvincing tank ruptures. An effort has been made to find a way of dealing with this issue.

The work done on issue 2 also addresses some errors in the current ADN 9.3.4 text and provides recommendations to remedy some ambiguities.

The following paragraphs give a summary of the results of the investigation. The full report on crash calculations can be found in the TNO report (ref [7]).

3.1 Approach

In order to investigate the sensitivity of the calculated results to the many choices and assumptions that need to be made for doing crash calculations, a systematic study has been carried out. For this purpose an inland waterway gas tanker was selected on which crash calculations were done. More than 35 simulations have been carried out in a combined effort by four different parties; Annmar Engineering, Damen Naval Engineering, Femto Engineering and TNO. The sensitivity study includes the following topics:

1. Friction.
2. Plasticity model.
3. Striking angle.
4. Striking location.
5. Tank pressure.
6. Failure criterion.
7. Mesh size.
8. Separate analysis of energy absorbing capacity and tank rupture.
9. The effect of the choice of software.

The ‘trapped structural material’ issue which manifests itself in case of topic 4, has been investigated by considering rupture of the tank and crashing of the ship structure separately. The idea is that this will yield more consistent results.

3.2 Main findings crash calculations

As an example, topic 4 (Striking location) is reported here. Figure 3.1 shows a typical collision scenario, in this example a V-shaped bow striking a gas tanker. The picture on the left shows the striking location in height. The picture on the right shows the observed damage at a penetration of 3.0 m. In the latter the striking bow and tank have been blanked. The point of view is looking from the inner side of the tank hold towards the lower half of the shell and the bottom.

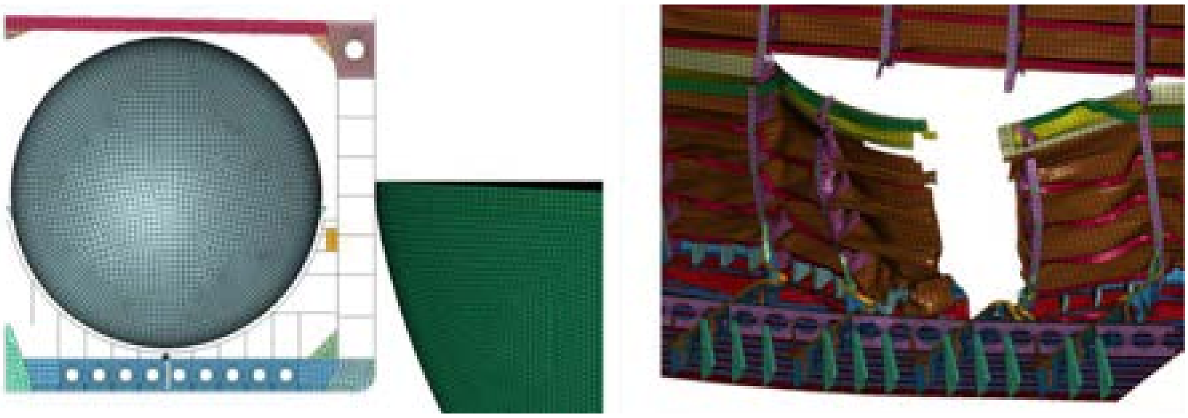

Figure 3.1 Typical collision scenario (left) and calculated damage ship structure, (right)

The calculated energy absorption versus penetration curves are shown in Figure 3.2. Four striking locations have been investigated:

1. Mid span between web frames, at stringer.
2. 50 mm forward of Mid span between web frames, at stringer.
3. Mid span between web frames, half stringer spacing below stringer.
4. 50 mm forward of mid span between web frames, half stringer spacing below stringer.

The drawn (—) vertical line indicates the penetration at which the tank fails in striking case 1, the dashed (-----) vertical line refers to striking case 2, the dotted (···) vertical line to striking case 3 and the dashed dotted line (-·-·-) to case 4. As expected, the energy absorption curve for the collision where striking at a stringer occurs lies above the curve for striking between two stringers. However, this effect is not accounted for in the current ADN regulations and could be both beneficial and detrimental depending on the layout of the ship structure with respect to the tank. The effect of a 50 mm shift of the longitudinal striking location is insignificant with respect to the energy absorption curve.

However, it is remarkable that in case of a collision at the stringer, the penetration at which tank rupture occurs shifts significantly, from 2.1 m to 1.8 m. With this shift the collision energy absorbing capacity changes as well. In case of striking between two stringers, rupture is calculated at a penetration of 1.6 m for both longitudinal positions.

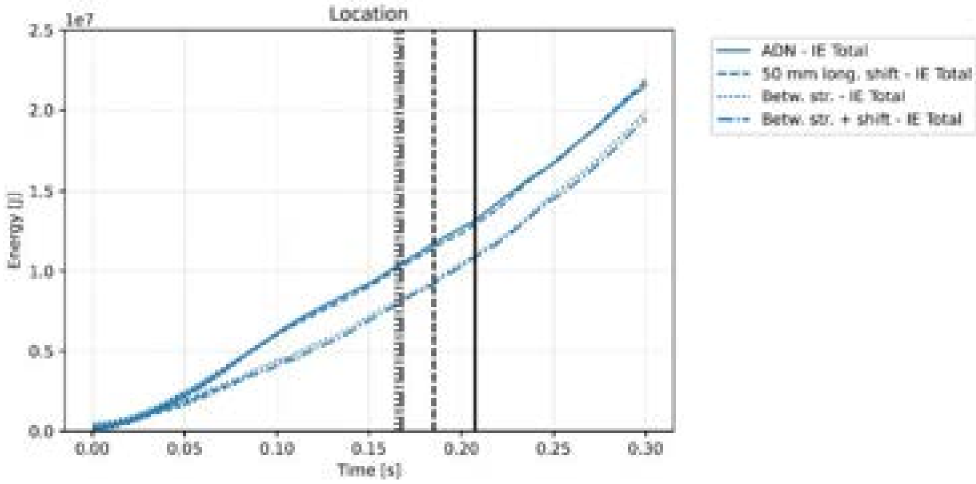

Figure 3.2 Typical collision energies absorbed and tank failure penetrations, two striking heights, effect of small longitudinal shift of striking location

3.3 Discussion

The example given illustrates that the effect of striking location variation may be different from expected. In case of a collision at a stringer, the calculations show a significant effect of a small (50 mm) shift of longitudinal striking location, which is not expected intuitively. This effect also affects the collision energy absorbing capacity and hence the probability of tank rupture for this collision scenario. It is unclear if this effect reflects reality or originates from the way the structural deformation is modelled numerically. This particular finding is considered unsatisfactory.

The other topics considered of the sensitivity study are addressed in the full report (ref [7]).

3.4 Recommendations

Regarding guidance for the crash calculations are the following recommendations:

1. The correct unit for exponential decay coefficient DC in the definition of the friction model in ADN 9.3.4.4.5.1 shall be provided (both 0.01 s/mm or 10 s/m are the correct coefficient with corresponding unit).
2. The plasticity model shall be described by a power law or equivalent representation discretised by at least 100 data points and up to a plastic strain of at least 1.
3. Additional locations of impact for type G tankers shall be included in the crash analysis: (i) the incoming bow first impacts the vessel at the stringer at mid tank height and (ii) the incoming bow first impacts the vessel between two stringers.
4. The maximum element size in the collision area shall be decreased to 100 mm in order to capture the deformed structure better.
5. Two initial tank pressures should be analysed for type G tankers: the minimum operating pressure of the tank and the maximum design pressure of the tank.
6. The failure model and criterion definition in article 9.3.4.4.4.1 shall be made non-ambiguous and the formula in 9.3.4.4.4.2 should be updated to match the currently accepted GL criterion.
7. It shall be clarified that failure in compression is excluded for the vessel structure.
8. As a general FEA requirement, ADN should require at least five through integration points and element deletion when at least half of the integration points have failed.
9. The crashworthiness calculations for the alternative construction should always be compared to crashworthiness calculations of a reference vessel with identical modelling approach, so that a consistent comparison can be made.
10. Element deletion based on damage accumulation shall be used in order to account for damage progression in an element.
11. Investigate a procedure where separate crash calculations are used to determine penetration at which tank rupture occurs and determine the energy absorbing capacity of the ship versus penetration. This may also be of interest for integrated tanks such as a membrane tank.

4 Issue 3: Effect analysis and exceeding 1000m3 limit

Section 9.3.4 also states a maximum allowable tank size of 1000 m^3. The question was raised whether this value could be increased because of the introduction of alternative fuels in inland waterway shipping, e.g. LNG and hydrogen, requiring dedicated tankers for transporting these fuels which would benefit from tanks exceeding this limit. The feasibility of increasing the maximum tank size beyond the current 1000 m^3 limit has been investigated through loss of containment effect analyses for tank sizes up to 5000 m^3.

4.1 Approach

In order to investigate the consequences of increasing the maximum allowable tank size beyond 1000 m^3, the effect of loss of containment has been calculated for various cargos. These analyses have been done for tank sizes ranging from 380 m^3 to 5000 m^3. Effect areas are compared for 1% lethality, based on toxicity, flame area, heat radiation and explosion overpressures. To be able to calculate these effect areas, modelling assumptions have to be made and these are conservative. The most important ones are:

1. Weather conditions: stable atmosphere and low wind speed, which means that the dispersion of gas clouds is slow resulting in higher concentrations. These conditions occur only during night time.
2. A large hole size of 2 m^2. This means that the outflow of liquids and gases from the tanks is relatively fast.
3. The position of the hole is taken at the bottom of the tank, and on the water level without ship structure. This leads to complete emptying of the tanks (with liquids) and complete outflow from the tank and the ship onto the water surface.
4. No dissolving of liquids in the water onto (or into) which it is spilled. This means that in the calculations, all of the spilled liquid evaporates from the water surface.
5. Clouds of flammable gas are ignited at the moment when their areas are at its largest (cloud fire) or the explosive mass is at its maximum (gas cloud explosions). Earlier or later moments of ignition would result in smaller effect areas.

The calculations were done with the software package EFFECTS (ref [3]) and are reported in full in ref [8].

4.2 Main findings maximum tank size limit

For illustration purposes propane is selected. Results of cloud fire calculations for different tank sizes are shown in Figure 4.1. The contours represent the flame area of the burning cloud if it is ignited at the moment that the cloud has its largest flammable area. It is observed that for all tank sizes the area exceeds the river limits. Notably, for 5000 m^3 tanks, the cloud can reach both sides of the river, while for the tank sizes between 380 and 1000 m³, the majority of the affected area is over water.

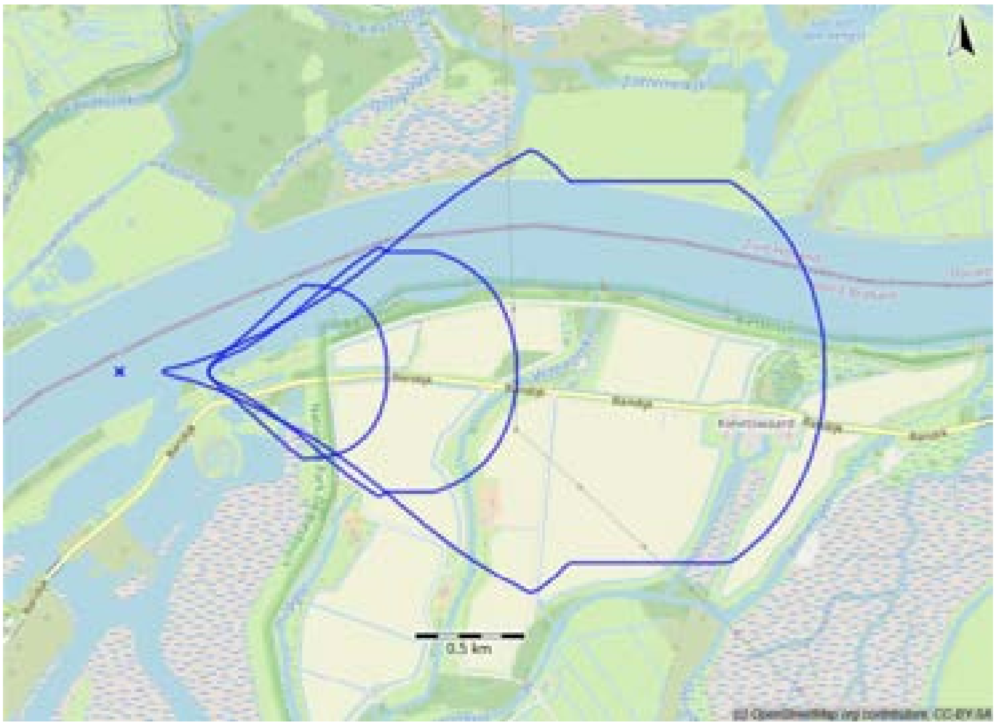

Figure 4.1 Propane – cloud fire contours for tank sizes 380, 1000 and 5000 m3.

Results for all substances are given in Figure 4.2. Effect areas vs. tank size are shown for all substances considered. The critical lethality criterium for each substance is shown in the legend. The largest effect area is the one for the propane cloud fire.

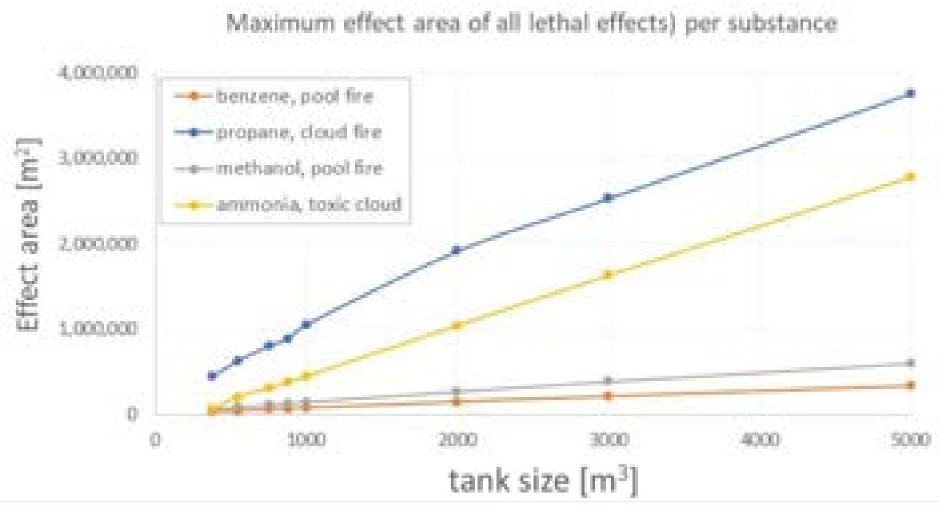

Figure 4.2 Largest effect area for all scenarios vs. tank size.

4.3 Discussion maximum tank size

For tank sizes up to 1000 m³, the rules as currently written in ADN 9.3.4 still hold. Doubling the tank volume results in almost doubling the effect area, and in most cases the affected area is over water.

For tanks larger than 1000 m³, the linear relation between tank volume and effect area remains more or less valid; the effect area sizes are slightly less than proportional to the tank size. The largest effect area occurs for the propane cloud fire and has a size of almost 4 km².

The effect area will reach the riverbanks in most cases and people on land will be affected as well. This is exacerbated by the fact that effect areas are not circular and not always centered around the release point and can cause hazards relatively far downwind from the release. This is especially the case for the toxic cloud of ammonia.

This study has looked at benzene, propane, methanol and ammonia. In the domain of transportation of fuels over inland waterways, there is also an increasing interest in LNG and in hydrogen. Some scenarios concerning accidents with LNG have already been investigated and published on the Scenarioboek EV (ref [4]). Using those scenarios and the assumptions of this study, similar calculations can be done to calculate effect areas for LNG. (Compressed) hydrogen is a very light gas and is therefore hard to model with current models implemented in EFFECTS that are aimed at neutral and dense gases. However, recent developments in EFFECTS' dispersion models will probably make it possible in the near future to model hydrogen accidents as well. Liquified hydrogen would involve also the outflow and evaporation analysis.

It is recommended for future work to incorporate LNG and liquid and compressed hydrogen as cargo.

4.4 Recommendation maximum tank size limit

In this effect study, it has been shown that areas beyond the riverbanks will also be affected when tanks larger than 1000 m³ would be used. Therefore, the risks associated with the use of larger tanks to transport hazardous chemicals is not acceptable without a more thorough risk evaluation that also involves the frequencies (probabilities) of accidents, the possible number of casualties (presence of population in the effect areas) and the specific substance being transported. Complete risk assessments are recommended in case tanks larger than 1000 m³ are proposed, addressing, among other aspects:

- Sailing routes
- Number of ship passages
- Tank size
- Hole sizes and positions with resulting outflow
- Substances to be transported
- Hazardous scenarios and mitigation measures
- Population densities along the waterways

5 Discussion, conclusions

5.1 Risk analysis framework

To be able to regulate the use of larger tanks with alternative fuels as cargo and other chemicals, a full-fledged risk analysis is recommended. Different countries have different frameworks for regulations of risks from transportation of hazardous goods. An example of such a framework is the Basisnet (ref [5]) which is applied in The Netherlands, and uses risk ceiling values for the 10^{-6} per year PR (*Plaatsgebonden Risico*: risk at specified location) value at the shore line. It is recommended that the ADN safety committee discusses what risk assessment framework is most suitable for ADN 9.3.4.

5.2 LNG and Hydrogen

As said in general it is recommended not to increase the general maximum limit of 1000 m^3 tanks. However it still may be acceptable to allow increased upper limits in case of specific cargos, especially LNG and hydrogen. In order to decide to develop an opinion on these specific cargos they should be analysed with respect to effect distances in case of a loss of containment in a similar fashion as referred to in this document. The framework of alternative designs as used in IGF may be a good starting point for a specific section in ADN. Such an approach requires the designers to address operational and incident scenarios, cargo characteristics and allowable consequences in a comprehensive manner for the specific ship and tank design.

5.3 Updates/ corrections ADN 9.3.4

Notwithstanding the above discussions, some updates are recommended to include on short notice. These recommendations are detailed in appendix A and include corrections, updates of data and solving ambiguities.

5.4 Alternative calculation method crashworthiness

In case independent tanks are applied, the energy absorbing capacity of ship structure and tank calculated in one model is challenging and may arouse many discussions. It is recommended to investigate a procedure where crash calculations are separated for tank and ship structure. Calculations performed on the tank are used to determine penetration at which tank rupture occurs and the ship structural analysis is used to determine the energy absorbing capacity of the ship versus penetration. This method may be useful for independent tanks, as well as integrated tanks such as membrane tanks.

6 Signature

TNO, May 2023

ValidSigned by Martijn Hoogeland
on 2023-05-25 16:08:45

M.G. Hoogeland
Author

ValidSigned by Caterina Lombardi
on 2023-05-25 16:09:03

C. Lombardi
Project Manager

ValidSigned by Tom Basten
on 2023-05-26 08:34:40

T.G.H. Basten
Research Manager Naval and Offshore Structures

Appendix A

Recommendation for updating section 9.3.4

	Section	*Proposed text amendment or modification*
9.3.4	**Alternative constructions**	
9.3.4.1	***General***	
9.3.4.1.1		**AMEND** However, in case of tanks intended for only one substance, of which it can be demonstrated that effect distances remain within a radius of 135 m from the outflow location in case of a loss of containment, larger tank capacities may be acceptable. The effect distance calculation method and assumptions made for the calculations are to be agreed upon with the recognised classification society.
9.3.4.2	***Approach***	
9.3.4.3	***Calculation procedure***	
9.3.4.3.1.2.2.2	Tank vessel type G	**REPLACE** For a tank ... be assumed. **WITH** For a tank vessel type G, three vertical collision locations shall be assumed; 1) at half tank height, 2) half stringer spacing below half tankheight and 3) half stringer spacing mm above half tankheight.
9.3.4.3.1.2.4.2	Tank vessel type G	**REPLACE** 1 . 3 = 3 **WITH** 3 x 3 = 9
9.3.4.3.1.3.2.2	Tank vessel type G	**REPLACE** The weighting factor .... location is assumed **WITH** The weighting factor for the each of the three vertical collision locations has the value of 0.333.
9.3.4.3.1.5.1		**REPLACE** Entire article. **WITH** For each collision energy absorbing capacity *Eloc(i)* , the associated probability of exceedance is to be determined. For this purpose the values for the cumulative probability density functions (CPDF) from the tables in 9.3.4.3.1.5.6 shall be used.
9.3.4.3.1.5.6		**REPLACE** Existing tables **WITH** Tables and text given in Appendix B.

	Section	Proposed text amendment or modification
9.3.4.4	***Determination absorbing capacity***	
9.3.4.4.1.1		**AMEND** The code shall also be capable of calculating and outputting (plastic) strain energy (energy by material deformation), friction energy and, in case of type G tankers, energy dissipated by tank deformation and fluid compression.
9.3.4.4.2.4		**REPLACE** 200 mm **WITH** 100 mm
9.3.4.4.2.5		**AMEND** Shell elements shall have at least 5 integration points through-thickness.
9.3.4.4.2.6		**REPLACE** In the FE …. option. **WITH** In the finite element calculation a suitable contact algorithm that includes self-contact shall be used. **DELETE** For this … FE-programs.
9.3.4.4.2.7		**NEW ARTICLE** *Tank vessel type G* For a tank vessel type G, the internal tank pressure shall be modelled by means of a compressible fluid volume. The initial pressure shall be set at max. design pressure of the tank.
9.3.4.4.3.1		**REPLACE** Ag = the ….and **WITH** Rm = ultimate tensile stress [N/m2] Ag = the uniform strain [-] at Rm **AMEND** The stress-strain relation shall be described by a power law directly or equivalent representation discretised by at least a 100 data points up to a plastic strain of 1.
9.3.4.4.3.2		**AMEND** Tensile test results are to be done in accordance with regulations from a recognised classification society.
9.3.4.4.3.3		**REPLACE** If only …value: **WITH** If only the ultimate tensile stress Rm is available, for shipbuilding steel with a yield stress not exceeding 355 [N/mm^2], the following approximation may be used in order to obtain the Ag value for a known ultimate tensile stress Rm with Rm in [N/mm^2]:

	Section	Proposed text amendment or modification
9.3.4.4.4	*Rupture criteria*	
9.3.4.4.4.1		**REPLACE** The first ... calculation steps. **WITH** The rupture of an element in a FEA is defined by the failure strain value. If the calculated strain, i.e. plastic effective strain, principal strain or the strain in the thickness direction, of this element exceeds its defined failure strain value at at least half of the through-thickness integration points, the element shall be deleted from the FE model. The deformation energy in deleted elements shall no longer change in subsequent calculation steps.
9.3.4.4.4.2		**AMEND** In order to avoid element deletion of elements in compression, rupture shall be ignored for all stress states with a triaxiality below -0.33, i.e. all stress states between equibiaxial compression and uniaxial compression.
9.3.4.4.4.6	Tank vessel type G	**REPLACE** Equivalent plastic … ignored. **WITH** In order to avoid element deletion of elements in compression, rupture shall be ignored for all stress states with a triaxiality below -0.33, i.e. all stress states between equibiaxial compression and uniaxial compression.
9.3.4.4.4.7		**NEW ARTICLE** *Tank vessel type G* Other rupture criteria for the pressure tank may be accepted by the recognised classification society if proof from adequate tests is provided.
9.3.4.4.5.1		***REPLACE*** DC = 0.01 ***WITH*** DC = 10 [s/m] ***REPLACE*** friction velocity ***WITH*** friction velocity [m/s].
9.3.4.4.5.2		**REPLACE** force penetration curves **WITH** energy-penetration curves
9.3.4.4.5.3.2		***REPLACE*** V_0 = volume **WITH** V_0 = vapour volume **REPLACE** V_1 = volume **WITH** V_1 = vapour volume
9.3.4.4.6.2		**REPLACE** extremely strong side structure **WITH** exceptionally stiff side structure

Appendix B
CPDF tables to be used in section 9.3.4.3.1.5

The probability for collision energies between the listed energy values shall be obtained through linear interpolation or by selecting the probability for the next higher energy listed.

The probability for collision energies between the listed effective mass values shall be obtained through linear interpolation or by selecting the probability density function for the next higher effective mass listed.

Table B.1: Cumulative probability density functions for collision energy.

	Effective mass of struck vessel											
	1500 tonne				2000 tonne				2500 tonne			
Energy_MJ	30% vmax	50% vmax	60% vamx	100% vmax	30% vmax	50% vmax	60% vamx	100% vmax	30% vmax	50% vmax	60% vamx	100% vmax
0	1.000	1.000	1.000	1.000	1.000	1.000	1.000	1.000	1.000	1.000	1.000	1.000
2	0.792	0.999	1.000	1.000	0.944	0.999	1.000	1.000	0.962	0.999	1.000	1.000
4	0.000	0.630	0.988	0.999	0.000	0.893	0.993	0.999	0.000	0.948	0.995	1.000
6		0.000	0.712	0.999		0.060	0.928	0.999		0.292	0.957	0.999
8			0.170	0.988		0.000	0.417	0.991		0.000	0.637	0.995
10			0.000	0.972			0.044	0.983			0.253	0.986
12				0.809			0.000	0.946			0.000	0.968
14				0.481				0.805				0.910
16				0.276				0.530				0.795
18				0.042				0.352				0.552
20				0.000				0.205				0.373
22								0.000				0.236
24												0.060
26												0.000

The probability for collision energies between the listed energy values shall be obtained through linear interpolation or by selecting the probability for the next higher energy listed.

The probability for collision energies between the listed effective mass values shall be obtained through linear interpolation or by selecting the probability density function for the next higher effective mass listed.

	Effective mass of struck vessel											
	3000 tonne				3500 tonne				4000 tonne			
Energy_MJ	30% vmax	50% vmax	66% vamx	100% vmax	30% vmax	50% vmax	66% vamx	100% vmax	30% vmax	50% vmax	66% vamx	100% vmax
0	1.000	1.000	1.000	1.000	1.000	1.000	1.000	1.000	1.000	1.000	1.000	1.000
2	0.979	0.999	1.000	1.000	0.981	0.999	1.000	1.000	0.982	0.999	1.000	1.000
4	0.000	0.961	0.996	1.000	0.000	0.969	0.997	1.000	0.000	0.976	0.998	1.000
6		0.447	0.969	0.999		0.574	0.980	0.999		0.652	0.981	0.999
8		0.000	0.812	0.995		0.058	0.851	0.996		0.189	0.887	0.997
10			0.412	0.986		0.000	0.514	0.988		0.000	0.610	0.988
12			0.063	0.979			0.238	0.981			0.316	0.982
14			0.000	0.942			0.000	0.954			0.058	0.958
16				0.850				0.910			0.000	0.920
18				0.683				0.824				0.842
20				0.530				0.643				0.701
22				0.355				0.500				0.590
24				0.249				0.338				0.466
26				0.070				0.240				0.330
28				0.041				0.070				0.232
30				0.000				0.044				0.065
32								0.000				0.044
34												0.000

The probability for collision energies between the listed energy values shall be obtained through linear interpolation or by selecting the probability for the next higher energy listed.

The probability for collision energies between the listed effective mass values shall be obtained through linear interpolation or by selecting the probability density function for the next higher effective mass listed.

	Effective mass of struck vessel											
	5000 tonne				8000 tonne				10000 tonne			
Energy_MJ	30% vmax	50% vmax	66% vamx	100% vmax	30% vmax	50% vmax	66% vamx	100% vmax	30% vmax	50% vmax	66% vamx	100% vmax
0	1.000	1.000	1.000	1.000	1.000	1.000	1.000	1.000	1.000	1.000	1.000	1.000
2	0.983	0.999	1.000	1.000	0.984	0.999	1.000	1.000	0.985	0.999	1.000	1.000
4	0.068	0.981	0.998	1.000	0.325	0.983	0.999	1.000	0.400	0.983	0.999	1.000
6	0.000	0.723	0.982	0.999	0.000	0.859	0.983	0.999	0.000	0.874	0.984	0.999
8		0.317	0.919	0.998		0.532	0.947	0.999		0.589	0.949	0.999
10		0.000	0.703	0.989		0.241	0.853	0.991		0.324	0.861	0.991
12			0.471	0.983		0.041	0.640	0.985		0.081	0.691	0.985
14			0.247	0.964		0.000	0.440	0.980		0.000	0.532	0.981
16			0.044	0.944			0.301	0.958			0.361	0.959
18			0.000	0.889			0.095	0.926			0.245	0.930
20				0.818			0.043	0.875			0.089	0.897
22				0.683			0.000	0.828			0.040	0.858
24				0.575				0.721			0.000	0.738
26				0.489				0.652				0.692
28				0.356				0.576				0.612
30				0.276				0.496				0.563
32				0.212				0.402				0.464
34				0.069				0.329				0.407
36				0.042				0.281				0.346
38				0.000				0.219				0.290
40								0.095				0.245
42								0.080				0.112
44								0.043				0.091
46								0.017				0.077
48								0.000				0.042
50												0.039
52												0.014
54												0.000

The probability for collision energies between the listed energy values shall be obtained through linear interpolation or by selecting the probability for the next higher energy listed.

The probability for collision energies between the listed effective mass values shall be obtained through linear interpolation or by selecting the probability density function for the next higher effective mass listed.

	Effective mass of struck vessel							
	12000 tonne				14000 tonne			
Energy_MJ	30% vmax	50% vmax	66% vamx	100% vmax	30% vmax	50% vmax	66% vamx	100% vmax
0	1.000	1.000	1.000	1.000	1.000	1.000	1.000	1.000
2	0.985	0.999	1.000	1.000	0.986	0.999	1.000	1.000
4	0.436	0.983	0.999	1.000	0.458	0.983	0.999	1.000
6	0.035	0.876	0.984	0.999	0.037	0.880	0.984	0.999
8	0.000	0.611	0.956	0.999	0.000	0.650	0.956	0.999
10		0.363	0.874	0.993		0.393	0.875	0.993
12		0.107	0.706	0.986		0.134	0.726	0.986
14		0.039	0.571	0.981		0.042	0.592	0.981
16		0.000	0.409	0.962		0.034	0.440	0.963
18			0.291	0.947		0.000	0.330	0.948
20			0.109	0.921			0.138	0.923
22			0.076	0.865			0.089	0.874
24			0.038	0.821			0.041	0.835
26			0.000	0.711			0.035	0.732
28				0.660			0.000	0.676
30				0.591				0.609
32				0.535				0.553
34				0.444				0.474
36				0.388				0.423
38				0.341				0.376
40				0.291				0.330
42				0.244				0.267
44				0.123				0.242
46				0.103				0.126
48				0.080				0.102
50				0.043				0.079
52				0.040				0.044
54				0.037				0.041
56				0.035				0.039
58				0.000				0.036
60								0.034
62								0.000

Mobility & Built Environment

Molengraaffsingel 8
2629 JD Delft
www.tno.nl

innovation
for life

Annex II

Molengraaffsingel 8
2629 JD Delft
The Netherlands

www.tno.nl

T +31 15 820 09 20

TNO report

TNO 2022 R12238

Background document: Updated ADN 9.3.4 collision energy statistics

Date	9 December 2022
Author(s)	Ir. M. L. Deul
Copy no	-
No. of copies	-
Number of pages	25 (incl. appendices)
Number of appendices	2
Sponsor	ADN 9.3.4 revision consortium
Project name	Revision ADN 9.3.4.
Project number	060.43088

Summary

ADN 9.3.4 prescribes how to demonstrate equivalent safety when a tanker is equipped with cargo tanks which exceed the ADN default maximum size of 380 m^3. For this purpose formulas are given for collision energies which a tanker is likely to be exposed to during a collision. The formulas are based on 1999 shipping statistics, which are outdated. Updated collision energies, based on more recent (2017) statistics have been derived and are reported in this document.

Underlying assumptions in the analysis are:

- Ship passings at Lobith are representative for inland shipping intensities.
- The utilization (average utilized cargo capacity) rate is 50% and the same for upstream and downstream passings.
- The collision is fully inelastic
- The struck vessel has zero speed

Proposed modifications to the collision energy formulation in the ADN entail:

- Updating the velocity distributions of the striking vessels based on reported characteristic (in this case maximum) speed of each vessel type, weighted against their quantity.
- Updating the displacement distributions based on actual registrations of vessel passages at Lobith in 2017

Most assumptions provide for a slightly conservative analysis, although the nett effect is not quantified. It is concluded that the collision energy available on the river Rhine to inflict damage, given a collision takes place, has increased significantly since 1999. The consequence in terms of required additional crashworthiness to keep complying with the intention of ADN regulation 9.3.4. is significant. Up to three times more energy should be absorbed by the struck vessel.

Contents

1 Introduction

The ADN regulations [1] (European Agreement concerning the international carriage of dangerous goods by inland waterways) is the governing agreement for shipping in European inland waterways. A part of this agreement is Chapter 9.3.4 on 'Alternative constructions', which describes the procedure for using tanks onboard inland waterway vessels larger than the maximum allowable volume of 380 m3 by limiting the probability of a leak of the tank. This chapter was introduced in 2005 and was based on the then available knowledge.

The project "revision ADN 9.3.4" has the objective to critically assess the standard from 2005 in light of novel shipping statistics and insights in crashworthiness and consequence analyses. The novel shipping statistics are reflected in a cumulative probability density function (CPDF) of the energy that is dissipated in case of a collision. Considering the trend of increasing vessel displacements over time and associated increase in dissipated energy, this CPDF needs to be updated. This part is presented in this report. The probability of exceeding the energy absorbing capacity of the vessel is the subject of another report [2].

1.1 Problem statement: requirement to update the ADN

Increased shipping intensity (both in terms of amount and individual displacements) has made the previously used energy distribution obsolete. An underestimation of the available collision energy poses an unsafe situation as vessels are deemed to withstand a collision with a certain amount of energy. Deviations in the available energy make this risk assessment invalid. Novel data sources provide an up-to-date and specific overview of the shipping intensity which thereby reflects a more accurate description of the potential collision energies that a vessel should be able to withstand.

1.2 Context: Maritime accidents in the Netherlands

To underline the importance of this analysis, the SOS database ("scheepsongevallen database") is consulted. This database collects the reported shipping accidents on the river Rhine, in the Netherlands. Between 2009 and 2018, 244 head-flank collisions between inland waterway vessels occurred. Additionally, there were 126 collisions of an inland waterway vessel with a jetty or dolphin. A total of 133 leaking vessels was reported. It should be noted that this list might not be complete and might not include accidents that were not significant enough to be reported.

Translated to history-based probabilities: The probability of having a head-flank collision or a vessel striking a jetty or dolphin, that is reported and listed in the SOS database, is approximately 1.87e-4 per vessel passage at Lobith, per year (once per 5600 years)[1], for the Dutch inland waterway network.

---

[1] Assuming that the registered 207456 passings at Lobith per year in 2017 are representative for the typical number of passings per year.

The probability of having a leaking vessel, that is severe enough to be reported and listed in the SOS database, in the inland waterway network of the Netherlands is approximately 6.41e-5 (once per 15600 years) per vessel passage at Lobith, per year.

1.3 Report contents

This report presents the updated energy distribution of encountered vessels, which substantiates the cPDF curves of dissipated energy in the ADN 9.3.4. These cPDF curves present the distribution of the dissipated energy in case of a collision with a predefined struck vessel.

The kinetic energy is expressed as $(1/2)\, mv^2$ where the v (sailing velocity) is discussed in Chapter 2, and the m (mass = displacement + added mass) is discussed in Chapter 3. Chapter 4 combines the velocity and mass to present the dissipated energy. Chapter 5 presents the comparison of the newly analyzed data with the current ADN 9.3.4. Specifically: In section 5.4 all above listed information is used to construct the cPDF curves of the dissipated energy for the example case of a 8000 tonnes struck vessel.

1.4 Main assumptions

Underlying assumptions in this analysis are:

- Ship passings at Lobith are representative for inland shipping intensities.
- The utilization (average utilized cargo capacity) rate is 50% and the same for upstream and downstream passings.

1.5 Goal of this document

This document aims to report the background information and substantiation for underlying choices for the newly proposed energy statistics for ADN 9.3.4. for future reference.

2 Sailing velocities

To determine the sailing velocities, two sources of information are compared: in Section 2.1 this is based on a datasheet of maximum sailing speeds per inland waterway ship types and in Section 2.2 this is based on an analysis of the distribution of sailing speeds per length and width class (roughly binned) **–** obtained from AIS data. The first one, based on inland waterway ship types/vessel characteristics is used in the proposed analysis.

2.1 Based on vessel characteristics

The German Bundesanstalt fur Wasserbau (BAW) published a list of typical inland waterway vessels on the River Rhine and other canals in Western Germany [3]. This report contains the typical values for the attainable ship speed at maximum engine power in both shallow (3m) and deep water (5m) for common ship types. The speed is given in STW (Speed Through Water, i.e. relative to the water body). The achievable ship speed is not reported for all vessels, but for the most common vessels. The maximum reported value in [3] is 18 km/h for deep water (5m) and 15 km/h for shallow water (3m)[2].

In appendix A this maximum attainable sailing speed is listed, per ship type. By only using the maximum sailing speed per vessel type, this analysis is deemed ***conservative.***

2.2 Based on AIS data registrations of 2019

In this section, all velocities are expressed as SOG (Speed over ground). By averaging the up- and downstream contributions the SOG = STW (Speed through water), under the assumption of a constant current. In the analysis in this report the STW is used: this is the speed at which vessels meet and the collision occurs (relative to the water body).

The source of information is the anonymized AIS data based on an analysis of Rijkswaterstaat [4] (Courtesy of Ernst Bolt [RWS] and Jan Hulskotte [TNO]). All ship passings at the Boven-Rijn, somewhat north-west of Lobith, are registered. For 2019 this were 26297 individual ships with in total 207456 passings (119307 upstream and 88149 downstream). This is approximately 53% more traffic (amount of passings) in 2019 than 1999. To anonymize the data, the passings are not reported individually. The mean, maximum, minimum and standard deviation of the velocity are reported for each ship class. Some of the datasets are tainted by unrealistically high maximum speeds (exceeding 100 km/h). However, due to the anonymization and combination of multiple datapoints in one bin, it is not possible to filter these out. The ship type classes (separated by width and length classes) used to anonymize the data are indicated in Table 1. The SK codes (inland shipping codes, see appendix A for the list) of inland shipping types that are presented by each bin are indicated in Table 2.

[2] The difference between deep and shallow water is attributed to the “squat effect” where the vessel will sink in deeper in shallow waters to compensate for the pressure reduction below the vessel, provided that the speed of the water in this contained area is higher. A vessel with a larger draft has a larger area and thereby more resistance.

Table 1: Width and length classes to categorize the ships

B1 < 7 m	L1 < 55 m
7 ≤ B2 < 9.6 m	55 m ≤ L2 < 86 m
9.6 ≤ B3 < 11.5 m	86 m ≤ L3 < 111 m
11.5 ≤ B4 < 17.2 m	L4 exceeding 111 m
B5 exceeding 17.2 m	

Table 2: Inland shipping types (SK codes) per length and width class

Downstream	L1	L2	L3	L4
B1	B01 M1 M2	B02 C1l	-	-
B2	-	B03 B04 M3 M4 M5	BI M6 M7	C2l
B3	C1b	-	BII-1 BIIa-1 M8	C3l BIIL-2 M9
B4	-	-	M10	BII-2L M11 M12
B5	-	-	C2b C3b	BII-4 BII-2B BII-6B BII-6L C4

It should be noted that the length and width classes in Table 2 contain a mix of vessel types (i.e. motor vessels, combi freighters and push barges).

2.2.1 Upstream statistics

The upstream velocity statistics are presented in Table 3 and Table 4.

Table 3: Upstream, average speed in km/h per inland shipping class

Upstream	L1	L2	L3	L4
B1	10.4	9.9	10.8	10.2
B2	10.9	10.8	10.8	7.9
B3	10.8	11.1	11.0	10.8
B4	10.8	11.5	11.1	10.9
B5	10.4	8.6	9.3	8.1

Table 4: Upstream, amount of registered passings per inland shipping class

Upstream	L1	L2	L3	L4
B1	60494	146	583	392
B2	3992	17623	1583	56
B3	2159	2478	9400	2431
B4	2051	106	7101	6057
B5	319	11	251	2074

2.2.2 Downstream statistics

The downstream velocity statistics are presented in Table 5 and Table 6.

Table 5: Downstream, average speed in km/h per inland shipping class

Downstream	L1	L2	L3	L4
B1	17.9	18.5	19.4	19.3
B2	18.9	18.2	18.7	15.5
B3	19.2	19.4	19.2	18.4
B4	19.3	20.3	19.5	18.8
B5	18.0	18.6	19.4	18.3

Table 6: Downstream, amount of registered passings per inland shipping class

Downstream	L1	L2	L3	L4
B1	35968	300	599	403
B2	1472	10563	2453	66
B3	1750	2111	9103	3095
B4	2117	97	7420	8041
B5	309	22	231	2029

2.2.3 Combined up- and downstream statistics

The combined average speed for up and downstream traffic, per length and width class, is indicated in Table 7. It is observed that the average sailing speed does not have a strong correlation with the vessel class.

Table 7: Average speed in km/h per length and width, average value over up- and downstream

Average	L1	L2	L3	L4
B1	14.2	14.2	15.1	14.7
B2	14.9	14.5	14.7	11.7
B3	15.0	15.3	15.1	14.6
B4	15.1	15.9	15.3	14.8
B5	14.2	13.6	14.4	13.2

To extract the representative Speed Through Water (STW) the average over up- and downstream traffic is calculated. The average velocity is 10.6 km/h for upstream passings and 18.5 km/h for downstream passages. The total average is a velocity of 14.4 km/h.

For reference, in [5] the current velocity on inland waterways is considered to have an up- and downstream variation of ± 3 km/h on average. The difference with the ± 4 km/h in the above analysis is attributed to the unrealistic extremes that influence the validity of the values: the AIS data reports maximum velocities above 50 km/h, which in turn affect both the mean and standard deviation per length and width class. This difference makes this analysis ***conservative***.

Table 8: Total vessel registrations of up- and downstream combined for 2019

Total	L1	L2	L3	L4
B1	96462	446	1182	795
B2	5464	28186	4036	122
B3	3909	4589	18503	5526
B4	4168	203	14521	14098
B5	628	33	482	4103

2.3 Comparison of available data sources

The two data sources: 1) vessel characteristics and 2) roughly binned AIS data are compared in Table 9.

Table 9: Comparison of available data sources for the sailing velocities

	Vessel characteristic (Section 2.1)	**Roughly binned AIS data (Section 2.2)**
Pro	+ Distinguish between ship types + Presents STW	+ Mean and standard deviation per length/width class
Con	– Only maximum is reported (conservative)	– SOG instead of STW – Data contains unrealistic extremes, affecting the mean and standard deviation – Does not allow for distinguishing ship types

From Table 9 it is observed that there are more cons to the use of the AIS data than pros. The only con of the use of the vessel characteristics is that the analysis might be conservative, as the vessels might sail at velocities below their characteristic value. The main significant downfall of using AIS data is that it presents the Speed Over Ground (SOG). Averaging the contributions of up and downstream traffic provides an average current of 4 km/h. However, the current is not constant over time (including fluctuations due to seasonal changes).

2.4 Conclusion

To conclude, the analysis will be based on the vessel characteristics. By doing this, ship types can be distinguished and the maximum STW for each ship type can be used. It is deemed acceptable that this source of information poses a conservative analysis.

3 Displacements

The mass of the vessel is obtained by summing the dry and added mass of the vessel. The dry mass is based on the displacement of the vessels, which are considered in this Chapter.

3.1 Source of information

The information on displacements is taken from the passage registrations at Lobith. For each passage a CEMT class is indicated, as well as the AIS draft. The data that is used is of 2017, for which the justification is presented in appendix B.

In this passage registry 10% of the ships is registered with a CEMT code, which means that the CEMT class of the other 90% is uncertain. To check the effect of this other 90%, a second source of information is used. This second source is the analysis of the future demand for berths at Lobith [6]. This analysis of the demand of berths is performed by assuming a percentage of passing ships that request berthing. The data is separated per CEMT class. This data is collected for 2012, and a prognosis for 2020 is made. Both distributions are compared to the distribution of CEMT classes in the 10% of registered CEMT classes in the 2017 dataset (see Figure 1).

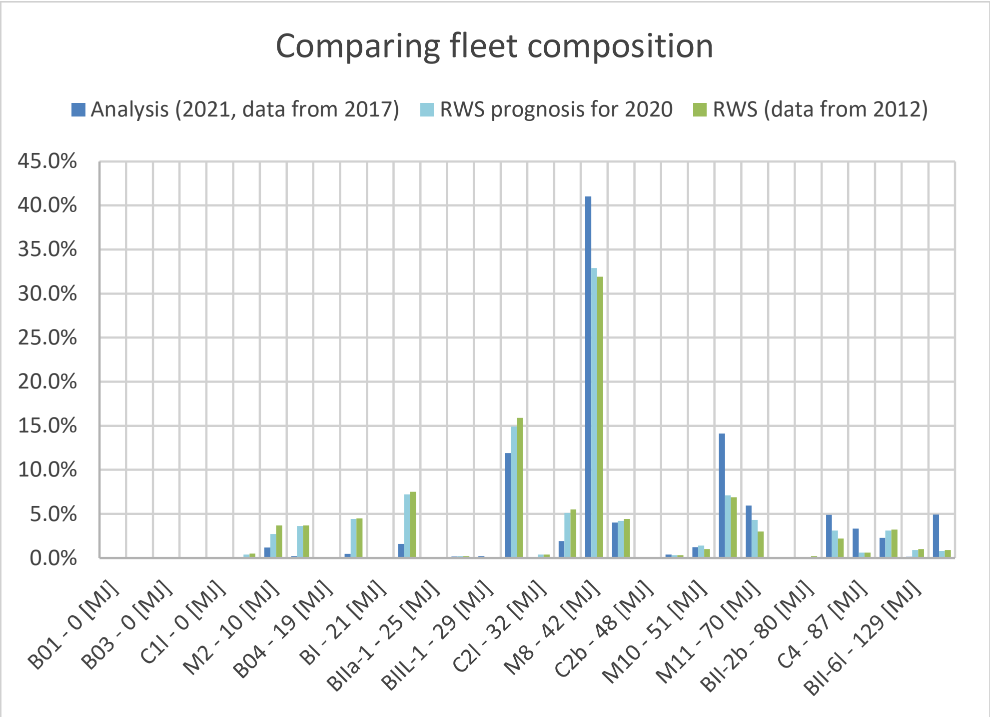

Figure 1: Comparing CEMT classes

Figure 1 shows that in the 2017 the contribution of the higher DWT vessels is over-estimated. This provides for a conservative analysis. It is concluded that the 2017 database (of individual passages) can be used, but adds ***conservatism***.

3.2 Analysis

The displacement of the inland waterway vessels is calculated using

$$\nabla = C_b \, L \, B \, T = 0.9 \, L \, B \, T,$$

in which ∇ is the displacement in m^3, C_b is the non-dimensional block coefficient (assumed equal to 0.9 for all vessels), L is the length between the perpendiculars in m, B is the ship width in m and T is the draft in m. The L and B are extracted from the inland shipping SK code that is assigned to each vessel (see appendix A for the properties per inland shipping class). The draft T is including in the passage registry for all datapoints individually.

All drafts of exactly 99 cm (assuming this is the Default value) are corrected to 3 meters. This value of 99 cm occurs most frequently for the BII-4, BII-6b, M6, M8 and M8 vessel. A mean maximum draft of those vessels is 3 m. This correction adds conservatism to the analysis because it assumes the maximum draft instead of the actual draft.

Combining the average sailing speed for the up- and downstream passings, this yields the following distribution of the displacement (see Figure 2).

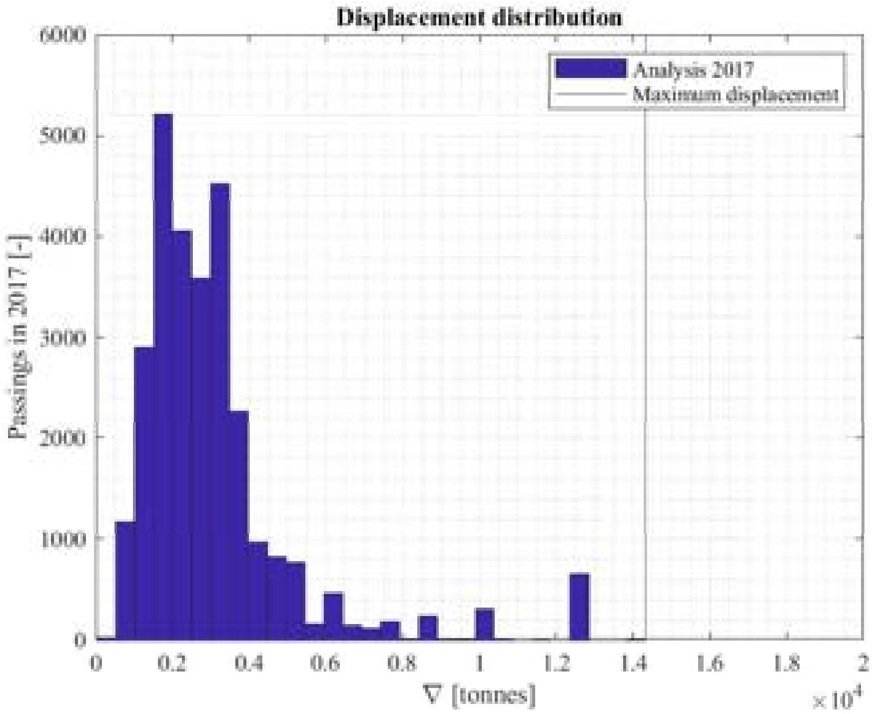

Figure 2: Displacement distribution (excluding added mass)

3.3 Conclusion

The approach to the displacements, as presented above, provides for a conservative estimate of the amount of high energy vessels, which are the vessels from which the critical collisions (i.e. imposing tank rupture) are expected. The confidence level for this estimation is deemed sufficient, based on the use of actual vessel registrations and the comparison between multiple sources of information.

4 Dissipated energy

The dissipated energy is derived in this Chapter. It is not proposed to make alterations to the ADN text in the formulation of the dissipated energy.

4.1 Derivation

In light of verifying the present ADN 9.3.4, the formula for the dissipated energy is derived. For this derivation it is assumed that there is a fully inelastic collision, neglecting a potential “bounce-back”. This yields a conservative assessment, since any elastic spring-back or skidding of the striking vessel is neglected and needs to be absorbed by the struck vessel.

The total energy that enters the system equals:

$$E_{in} = \frac{1}{2} m_a v_{a,1}^2 + \frac{1}{2} m_b v_{b,1}^2$$

Conservation of momentum yields:

$$v_2 = \frac{m_a v_{a,1} + m_b v_{b,1}}{m_a + m_b}$$

$$E_{out} = \frac{1}{2}(m_a + m_b) v_2^2 = \frac{1}{2}(m_a + m_b)\left(\frac{m_a v_{a,1} + m_b v_{b,1}}{m_a + m_b}\right)^2 = \frac{\frac{1}{2}\left(m_a v_{a,1} + m_b v_{b,1}\right)^2}{m_a + m_b}$$

$$E_{diss} = E_{in} - E_{out} = \boldsymbol{\frac{1}{2} m_a v_{a,1}^2 + \frac{1}{2} m_b v_{b,1}^2 - \frac{\frac{1}{2}\left(m_a v_{a,1} + m_b v_{b,1}\right)^2}{m_a + m_b}}$$

Assuming the struck vessel is not moving $v_{b,1} = 0$, yielding:

$$E_{diss} = E_{in} - E_{out} = \frac{1}{2} m_a v_{a,1}^2 - \frac{\frac{1}{2} m_a^2 v_{a,1}^2}{m_a + m_b} = \frac{1}{2} m_a v_{a,1}^2 \left(1 - \frac{m_a}{m_a + m_b}\right) = \boldsymbol{\frac{1}{2} m_a v_{a,1}^2 \left(\frac{m_b}{m_a + m_b}\right)}$$

This is the same formula as listed in the ADN 9.3.4.

Considering that for a $m_b \rightarrow 0$ this provides $E_{diss} \rightarrow 0$, which is correct considering no energy is dissipated in case of no collision.

<u>**Important note:**</u> In the existing ADN the struck vessel has no speed. This assumption is correct for the transverse collision. When the striking vessel has an angle with the struck vessel, it is also likely that the struck ship has forward speed. This may be more stringent.

4.2 Conclusion

It is proposed to not deviate from the approach in the ADN. That means: the velocity of the struck vessel is zero and the mass of the struck vessel is selected from a predefined list of masses. For each mass category the cPDF line is presented.

The assumption of the fully inelastic collision is a conservative assumption whereas the assumption that the struck vessel has no speed is unconservative. The nett effect of both assumptions is not known.

5 Comparison to ADN 9.3.4. (2005)

The original document of the ADN is from 2005. The energy statistics were obtained from the Rijkswaterstaat reference [7] of 1999. However, with time the shipping intensity has increased. The current approach with the data as presented in this document is compared to the 2005 analysis to indicate the main implications.

5.1 Fleet composition

The fleet composition for both the 2005 and current analysis is based on deadweight classes as used in the original ADN 9.3.4. These classes are obtained from [7]. Figure 3 presents the comparison between the original DWT classes from 1999 and the translation of the logged data of 2017. Table 10 contains the DWT class categories.

Table 10: DWT class categories, according to [7]. All DWT in tonnes.

DWT class	Min DWT	Max DWT	DWT class = Bin average DWT + 10% (added mass)
149	21	250	149
358	250	400	358
578	400	650	578
908	650	1000	908
1375	1000	1500	1375
1925	1500	2000	1925
2750	2000	3000	2750
6250	3000	8400	6270

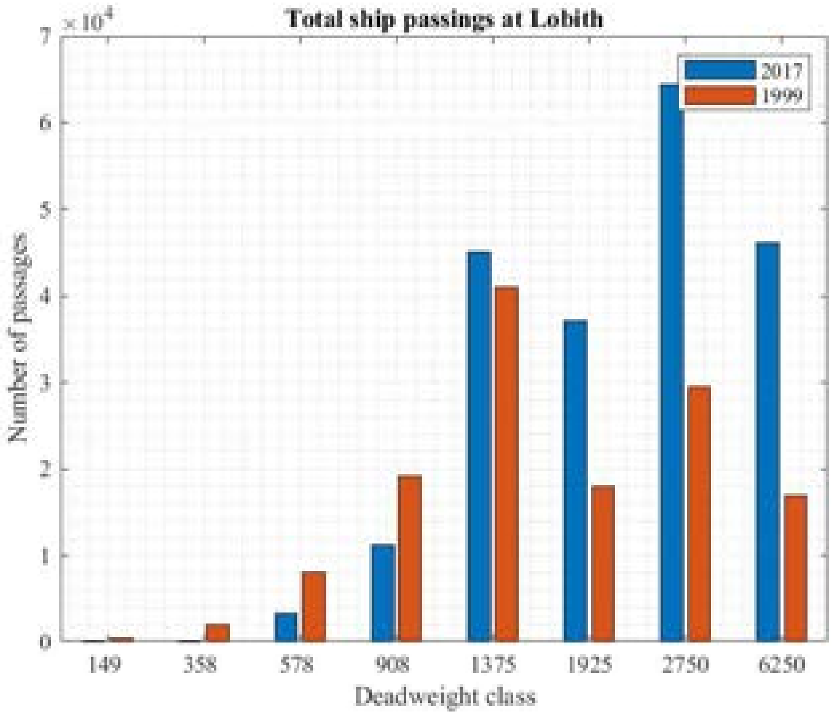

Figure 3: DWT classes of 1999 and 2017 (expressed in the bins as used in the 1999 analysis [8]

It is observed that the total activity (amount of passages) on this sailing route has significantly increased in 23 years. Besides that, the average DWT of the inland waterway vessels has increased as well.

5.2 Sailing velocities

In the 2005 update of ADN 9.3.4, the sailing velocity is obtained by fitting a line through datasets of the trial velocities of inland waterway vessels. This is in part due to the lack of data on the actual speeds at the time. Accounting for the fact that the trial speed is typically at 100% MCR, whereas the service conditions are at approximately 90% MCR, the service speed is taken at 1 km/h below the trail speed in [8].

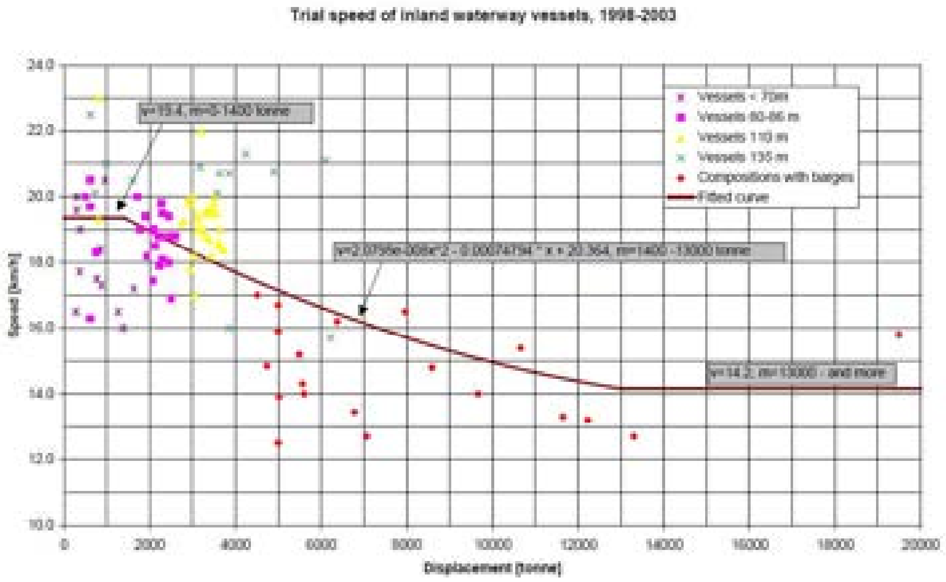

Figure 4: Fitted curve of the trial speed of inland waterway vessels [8]

However, the actual speed of the vessels on the inland waterway network of the Netherlands is on average 14 km/h for all inland shipping classes.

To compare the resulting available energy distributions it should be noted that the data in [8] is presented per DWT class. Not all DWT classes have the same bin width (see Figure 3). In the present analysis the bin width is constant; providing for a more smooth and continuous expression. Figure 5 shows both the cPDF and pdf of the available kinetic energy -not considering a struck vessel- for the 1999 data (Reference ADN 9.3.4.) and the present analysis. The same trend as in Figure 3 is observed: in 1999 more “low kinetic energy” vessels were sailing on the inland waterway routes.

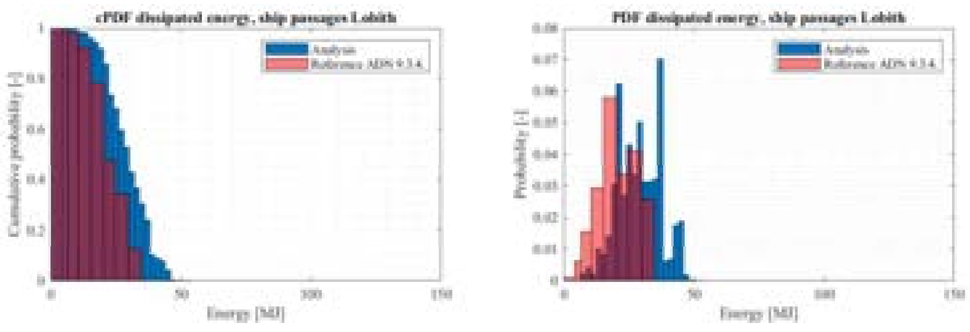

Figure 5: Comparing the kinetic energy data of 1999 and 2017 in a normalised (cumulative) histogram for the river Rhine

5.3 Main differences in approach and input

The main differences between the 2005 and current analysis are:

- The use of the actual draft T to estimate the actual displacement per passing instead of considering 1.25 times the maximum DWT (i.e. always sailing with the maximum DWT loaded, which is conservative).
- The use of novel statistics (increased inland shipping intensity)
- The use of more precise bins instead of roughly binned DWT classes to determine the shipping intensity.

5.4 Example for 8000t struck vessel [full speed]

8000 tonnes	
E coll	CPDF
[MJ]	[ ]
3.39	1.000
5.37	0.999
7.35	0.999
9.34	0.995
11.32	0.986
13.30	0.982
15.28	0.962
17.26	0.946
19.25	0.918
21.23	0.858
23.21	0.734
25.19	0.680
27.17	0.595
29.16	0.529
31.14	0.429
33.12	0.367
35.10	0.305
37.09	0.241
39.07	0.102
41.05	0.089
43.03	0.076
45.01	0.041
47.00	0.004
48.98	0.001
50.96	0.000
52.94	0.000

The figure below presents the example diagram for a struck vessel with a total displacement of 8000 tonnes with no initial speed for both the 2005 and 2021 analysis. This diagram shows that the novel analysis includes more high-tonnage vessels, exhibited as an increase in the tail of the diagram. In the 2005 analysis the highest collision energy was 31 MJ. In the 2021 analysis this is 38 MJ (for a fully effective BII-6b combination sailing at 14 km/h with 2.1 m draft). Besides that the probability of dissipating energies below 28 MJ has reduced. This is due to the use of actual drafts and speeds, instead of conservatively assuming all vessels fully loaded and sailing at 90% of their trial speed.

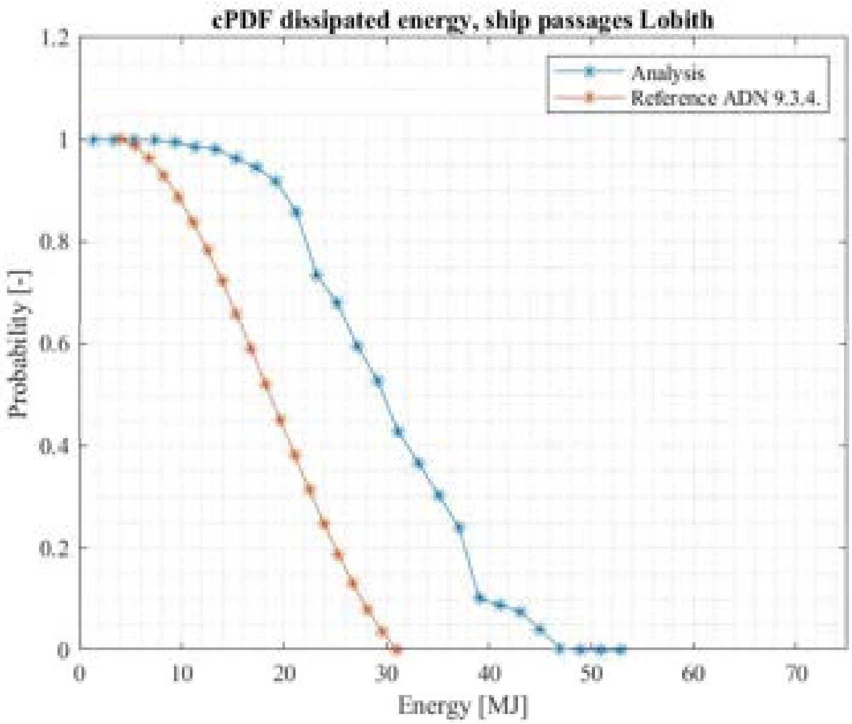

Figure 6: cPDF comparison collision energy, struck vessel of 8000 tonne, comparing 2017 and 1999 statistic

The table on the left side presents the numerical values of the cPDF line of the current analysis.

As expected the available collision energy has clearly increased since 1999. When an ship owner wants to have a tanker built with cargo tanks exceeding the default ADN maximum size of 380 m³, the owner needs to decrease the probability of tank rupture in case of a collision. Should the owner want to use tanks of say 760 m³, i.e. 2 times 380, the probability of tank rupture must be reduced by a factor 2 compared to a ship designed in compliance with the prescriptive regulations for scantlings according ADN (the minimum scantlings design or reference design).

For example, suppose the reference design can absorb 22 MJ up to tank rupture. According to the data from 1999, the probability of tank rupture, given a collision, is approx. 0.32. The new design would require a reduced probability of tank rupture of 0.16. Using the CDF curve from 1999, this results in a required energy absorbing capacity of 26 MJ. Performing the same exercise based on the current updated curve yields; (i) probability of tank rupture for the reference design of 0.8, (ii) a required reduced probability for the new vessel of 0.4, i.e. (iii) a required energy absorbing capacity of 32 MJ.

It is noted that the CPDF based on updated (2017) data shows a remarkable knuckle (in the 8000 tonne example at 39 MJ). This is caused by the presence of ships in the 10000 - 15000 tonne effective mass range. This cannot be described conveniently with a simple formula, as is currently used in ADN 9.3.4. Therefore it is proposed to express these curves in the updated ADN 9.3.4 text through tabled values instead of a formula. Intermediate values can be determined through linear interpolation.

6 Conclusion

The recommended approach to updating the energy curves in ADN 9.3.4 is reported in this document.

The underlying assumptions are:
- Ship passings at Lobith are representative for inland shipping intensities.
- The utilization (average utilized cargo capacity) rate is 50% and the same for upstream and downstream passings.
- The collision is fully inelastic.
- The struck vessel has zero speed.

The distribution of the velocities of the striking vessels is based on the reported characteristic (in this case maximum) speed of each vessel type. This assumption poses a conservative estimate of the available energy of the striking vessel considering that vessels do not always sail at their maximum speed.

The distribution of displacements is based on actual registrations of vessel passages at Lobith in 2017. The vessel registrations indicate more large (i.e. high energy) vessels than the RWS prognosis, although the implication of this is deemed limited.

There is no change proposed for the formulation of the dissipated energy. The assumption of the fully inelastic collision is a conservative assumption whereas the assumption that the struck vessel has no speed is unconservative. The net effect of both assumptions is not known.

6.1 Discussion

As expected the collision energy available on the river Rhine to inflict damage, given a collision takes place, has increased significantly since 1999. The consequence in terms of required additional crashworthiness to keep complying with the intention of ADN 9.3.4. is significant. For a single example, an 8000 tonnes tanker, the required increase of crashworthiness is 6 MJ. The current regulations requires for this example an increase from 22 MJ to 26 MJ, i.e. 4 MJ, whereas with the updated CPDF data the required increase would be from 22 MJ to 32 MJ, i.e. 10 MJ.

7 References

[1] United Nations Economic Commission for Europe; Committee on Inland Transport, "European Agreement concerning the international carriage of dangerous goods by inland waterways," 2021.

[2] N. Werter and O. Coppejans, "TNO 2022 R11532 ADN 9.3.4 FE Sensitivity Analysis," TNO, Delft, the Netherlands, 2022.

[3] BAW, "Driving Dynamics of Inland Vessels: Vessel Behaviour on European Inland Waterways and Waterway Infrastructure with Special Respect to German Waterways," BAW, Karlsruhe, Germany, 2016.

[4] Rijkswaterstaat, *Database AIS snelheden binnenwater 2019,* 2021.

[5] R. G. Hekkenberg, "Inland Ships for Efficient Transport Chains," Delft University of Technology [PhD Thesis], 2013.

[6] Rijkswaterstaat, "Toekomstige Ligplaatsbehoefte Overnachtingshaven Lobith 2013," Rijkswaterstaat, Delft, 2013.

[7] Ministerie van Verkeer en Waterstaat, Directoraat Generaal Rijkswaterstaat, "Nederland en de scheepvaart op de binnenwateren," ISSN 1566-1164, 1999.

[8] TNO, "Background document to the Guideline for acceptance of cargo tanks larger than sizes which are in accordance with ADNR(2005)," 2005.

[9] Rijkswaterstaat, Adviesdienst Verkeer en Vervoer, "Classificatie en kenmerken van de Europese vloot en de Actieve vloot in Nederland," Rijkswaterstaat, Rotterdam, 2002.

[10] CCNR (Central Commission for the Navigation of the Rhine), "Inland navigation in Europe - Market Observation," CCNR, 2016.

[11] NEA, "Factorkosten van het goederenvervoer, een analyse van de ontwikkeling in de tijd," 2004.

[12] Rijkswaterstaat, "Waterstanden," Rijkswaterstaat, [Online]. Available: https://www.vaarweginformatie.nl/frp/main/#/hydro/water_level. [Accessed 28 October 2021].

8 Signature

Delft, December 2022 TNO

ValidSigned by Marije Deul
on 2022-12-12 15:43:44

ValidSigned by Martijn Hoogeland
on 2022-12-12 15:18:01

ir. M. L. Deul
Author

ir. M. Hoogeland
Project Manager

ValidSigned by Tom Basten
on 2022-12-21 12:04:22

dr.ir. T.G.H. Basten
Research Manager Structural Dynamics

A Inland shipping classification: properties per SK code

Total registrations in 2017 = 30499.

Table 11: Classification of inland shipping types, considering both the SK code and CEMT class for reference [9]. The length L and width B are the average of the SK code category. The maximum STW is taken from based on the data from the BAW [3], where bold font numbers indicate exact values. The non-bold font values are based on values in adjacent cells.

SK code	Amount	Description (Dutch)	CEMT class	B [m]	L [m]	V max [km/h]
B01	0	Duwstel	I	5.2	55	**14**
B02	0	Duwstel	II	6.6	65	14
B03	0	Duwstel	III	7.5	80	14
B04	3	Duwstel	III	8.2	85	14
BI	15	Europa I duwstel	IV	9.5	95	14
BII-1	45	Europa II duwstel	V a	11.4	102.5	14
BII-2b	1	2-baksduwstel breed	VI a	22.8	120	**14**
BII-2L	4	2-baksduwstel lang	V b	15.1	180	**16**
BII-4	655	4-baksduwstel	VI b	22.8	190	**14**
BII-6b	1417	6-baksduwstel lang (incl 5-baks breed)	VII a	34.2	195	13
BII-6l	34	6-baksduwstel lang (incl 5-baks lang)	VI c	22.8	270	**13**
BIIa-1	2	Europa IIa duwstel	V a	11.4	101	14
BIIL-1	58	Europa II Lang	V a	11.4	130	14
C1b	0	2 spitsen breed	I	10.1	38.5	14
C1l	0	2 spitsen lang	I	5.05	78.5	14
C2b	3	Klasse IV + Europa I breed	VI a	19	95	14
C2l	15	Klasse IV + Europa I lang	IV b	9.5	177.5	14
C3b	111	Klasse Va + Europa II breed	VI a	22.8	102.5	14
C3l	1155	Klasse Va + Europa II lang	V b	11.4	180	14
C4	949	Klasse Va + 3 Europa II	VI b	22.8	185	14
M1	1	Spits	I	5.05	38.5	**12**
M10	351	Maatgevend schip 13,5 * 110 m	VI a	13.5	110	18
M11	1700	Maatgevend schip 14,2 * 135 m	VI a	14.2	135	18
M12	1401	Rijnmax Schip	VI a	17	135	18
M2	340	Kempenaar	II	6.6	52.5	**16**
M3	63	Hagenaar	III	7.2	62.5	**18**
M4	128	Dortmund Eems	III	8.2	70	18
M5	453	Verlengde Dortmund	III	8.2	82.5	18
M6	3416	Rijn-Herne Schip	IV	9.5	92.5	18
M7	548	Verlengde Rijn-Herne	IV	9.5	105	18
M8	11762	Groot Rijnschip	V a	11.4	111	**18**
M9	4049	Verlengd Groot Rijnschip	V a	11.4	135	**18**

B Context of inland shipping transport to justify 2017 as a representative year for the analysis

CONTEXT INLAND SHIPPING TRANSPORT
MAIN EVENTS PER YEAR

- 2017: market was quite stable and favorable
  - "Alles bij elkaar genomen wijst dit voor het goederensegment op een gunstiger economisch klimaat in 2017 dan een aantal jaren geleden." (CCR Marktobservatie - Jaarverslag 2018)
- 2018: low waterlevels
  - "De laatste twee dalingen zijn ten gevolgen van de lange extreme droogte die 2018 en 2019 kenmerkten." (binnenvaartcijfers.nl, Vervoerd gewicht binnenvaart – Binnenvaartcijfers)
  - "2018 stond voor de Europese binnenvaart in het teken van de aanhoudende lage waterstanden in de tweede helft van het jaar die van invloed waren op verschillende economische parameters." (CCR Marktobservatie - Jaarverslag 2019)
- 2019: low waterlevels and macro-economics not beneficial
  - "De algemene macro-economische randvoorwaarden in 2019 maakten het voor de binnenvaartsector moeilijk om de vervoersvolumes te vergroten." (CCR Marktobservatie - Jaarverslag 2020)
  - "De laatste twee dalingen zijn ten gevolgen van de lange extreme droogte die 2018 en 2019 kenmerkten." (binnenvaartcijfers.nl, Vervoerd gewicht binnenvaart – Binnenvaartcijfers)
- 2020: COVID-19
  - "De gevolgen van de pandemie voor de economische activiteit waren merkbaar in de gehele vervoerssector en de binnenvaart vormt zeker geen uitzondering daarop." (CCR Marktobservatie - Jaarverslag 2021)

FLEETDEVELOPMENTS
PER FREIGHTER SIZE

- Source: CBS
- Increase in *large* freighters, decrease in vessels up to 2000 ton
- In 2010:
  - 2536 vessels up to 1000 tonnes
  - 1280 between 1000 and 2000 tonnes
  - 943 between 2000 and 3000 tonnes
  - 623 exceeding 3000 tonnes
- *How to explain the increase in 2000-3000 tonners in 2019?*
  - Mostly attributed to the delivery of newbuilt vessels
  - 20 new dry bulk vessels, 42 new tankvessels (NL registered) added to fleet in 2019 (CCR, 2020). These were ordered upon economic recovery in 2014 ("2014 was het jaar van economische herstel" – de Volkskrant 26-03-2015).

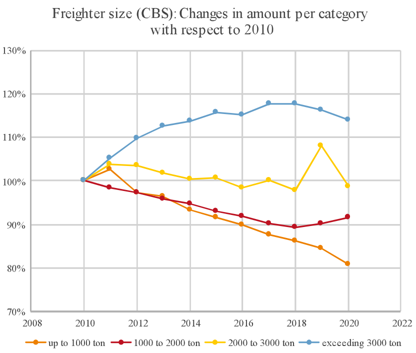

PROGNOSES
ACCORDING TO CPB AND PANTEIA ANALYSES

- CPB prognosis from 2011, not including the effects of COVID-19
  - High = economic growth, high migration saldo, high (technological) development rates, low price for energy, substantial climate policy
  - Low = limited economic growth, low migration saldo, slower (technological) development rates, high price for energy, limited climate policy
- Panteia (2020): report on the effects of the COVID-19 pandemic on the inland shipping tonnage prognosis
  - BR = "basis raming": (too) positive outlook
  - DD = "diep dal": accounting for multiple rounds of measures
  - In 2020 more tonnes/year transported than predicted by BR scenario Panteia
  - Correction is using the same change-percentages, but accounting for real 2020 data

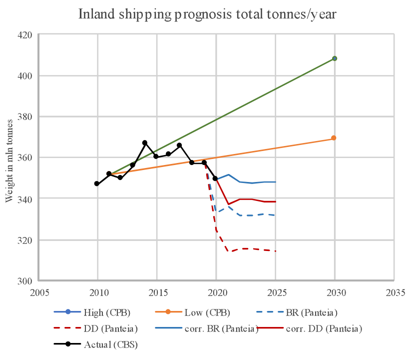

CONCLUSION
SELECTING 2017 AS REPRESENTATIVE YEAR

- 2017 was a considerably good year for inland shipping in terms of total transported DWT
  - Thus slightly conservative
- 2018 and 2019 are considerably bad years due to low waterlevels
- 2020 and 2021 are highly influenced by the COVID-19 pandemic

- The 2017 data is selected
  - Medium term (10 years): conservative
  - Long term (>10 years): a good estimate, according to a combination of the prognoses from Panteia (medium term, accounting for COVID-19) and CPB (long term prognosis, written before COVID-19)